Viscoelastic Properties of Natural Rubber Composites Reinforced by Defatted Soy Flour and Carbon Black Co-Filler

L. Jong

United States Department of Agriculture, National Center for Agricultural Utilization Research, Agricultural Research Service, Peoria, Illinois 61604

Received 16 November 2006; accepted 6 May 2007
DOI 10.1002/app.26851
Published online 22 August 2007 in Wiley InterScience (www.interscience.wiley.com).

ABSTRACT: Filler mixtures of defatted soy flour (DSF) and carbon black (CB) were used to reinforce natural rubber (NR) composites and their viscoelastic properties were investigated. DSF is an abundant and renewable commodity and has a lower material cost than CB. Aqueous dispersions of DSF and CB were first mixed and then blended with NR latex to form rubber composites using freeze-drying and compression molding methods. A 40% co-filler reinforced composite with a 1 : 1 DSF : CB ratio exhibited a 90-fold increase in the rubber plateau modulus compared with unfilled NR, showing a significant reinforcement effect by the co-filler. The effect, however, is lower than that observed in the carboxylated styrene–butadiene rubber composites reported earlier, indicating a significant effect from the rubber matrix. The co-filler composites have elastic moduli between those of DSF and CB reinforced composites. Stress softening and recovery experiments indicated that the co-filler composites with a higher CB content tend to have a better recovery behavior; however, this can not be simply explained from the recovery behaviors of the single filler (DFS and CB) composites. CB composites prepared by freeze-drying show a strain-induced reorganization of fillers. Strain sweep experiment data fit with the Kraus model indicates the co-filler composites with a higher CB content are more elastic, which is consistent with the recovery experiments. © 2007 Wiley Periodicals, Inc. J Appl Polym Sci 106: 3444–3453, 2007

Key words: rubber; composites; reinforcement; viscoelastic properties; defatted soy flour

INTRODUCTION

Natural rubber (NR) is one of the most important elastomeric materials for diverse industrial applications. However, NR by itself does not possess a high enough modulus for most applications and needs to be reinforced with fillers and crosslinked with curing agents. Two major reinforcing fillers used today are fumed silica and carbon black (CB). Fumed silica has a higher cost than CB. CB is mainly derived from aromatic oil in petroleum or from natural gas. Substitution of CB with renewable fillers has been investigated in recent years. Recent studies have reported the modulus enhancement of rubbers by natural materials, for example, oil palm wood,[1] crab shell chitin,[2] bamboo fiber,[3] and soybean products.[4–7] The use of renewable protein in rubber latex to form composites was also reported in a few patents[8–10] and can be traced back to the 1930s. For example, Lehmann and coworkers had demonstrated the use of casein (milk protein) in NR latex to achieve approximately a 4-fold increase in the modulus.[10] Protein as an additive in rubber materials has also been claimed to improve the antiskid properties of winter tread tires.[11–13] In rubber reinforcement, factors such as aggregate structure, effective filler volume fraction, filler-rubber interaction, and the elastic modulus of filler clusters all have an important impact on the moduli of rubber composites.[14] Mechanically, the elastic modulus of base rubber is not significant when compared with the modulus of the filler network in highly filled elastomeric composites.[15] In some of practical applications, the issue of moisture sensitivity is always associated with natural materials, but it may be improved through product formulation and/or selective applications. For example, it may be used as a component in multi-layered structures, in coated objects, in elevated temperature applications or in a rubber part formulated with a hydrophobic plasticizer.

Defatted soy flour (DSF) is a soy product after soybean oil is removed from soybean flakes. It is an abundant and inexpensive renewable commodity. The composition of DSF includes soy protein, soy carbohydrate (insoluble carbohydrate), and soy whey (soluble carbohydrate).[16] Structurally, soy protein is a globular protein and its aggregates are simi-

Names are necessary to factually report on available data; however, the USDA neither guarantees nor warrants the standard of the product, and the use of the name by USDA implies no approval of the product to the exclusion of others that may also be suitable.

Correspondence to: L. Jong (lei.jong@ars.usda.gov).

Journal of Applied Polymer Science, Vol. 106, 3444–3453 (2007)

lar to colloidal aggregates, but soy carbohydrate is a nonglobular, film-like material.[4] DSF also has the lowest cost compared with soy protein concentrate and soy protein isolate because it is the raw material for the production of these soy products. DSF is also economically more favorable than CB. Previously, DSF was used to reinforce styrene–butadiene (SB) rubber and indicated a significant reinforcement effect in the small strain region.[4] Previous studies also have indicated the importance of the interaction between filler and matrix.[14] In this study, NR latex instead of SB is used as the rubber matrix to gain more information on its effect. The objective of this investigation is therefore to explore the co-filler effect by using a mixture of DSF and CB as reinforcement fillers and observe their effects in the NR matrix.

EXPERIMENTAL

Materials

The DSF (Nutrisoy 7B) used in this research was a spray dried powder (Archer Daniels Midland Company, Decatur, IL). The DSF contains ~ 53% soy protein and has a protein dispersibility index (PDI) of ~ 90. Sodium hydroxide, used to adjust pH, was ACS grade. Aqueous dispersion of CB *N*-339 (Sid Richardson Carbon Co.) was prepared by dispersing ~ 100 g of CB in water with the aid of a surfactant, sodium lignosulfonate (Vanisperse CB, Lignotech, Rothschild, WI). The weight fraction of the surfactant based on CB is 3%. The dispersion was homogenized at 10^4 rpm for 1 h. The resulting CB dispersion had a solid content of 10.9%. The NR latex used was HARTEX® 101 obtained from Firestone Polymers (Akron, OH). The glass transition temperature of crosslinked NR with 3 phr (parts per hundred parts of rubber) sulfur is −56°C (determined by G'' maximum). The NR latex received had ~ 60% solids and a pH ~ 10. The volume weighted mean particle size of the latex was ~ 0.85 μm. The size distributions of DSF, CB, and NR aggregates are shown in Figure 1. An aqueous dispersion of sulfur (Bostex 410) was obtained from Akron Dispersions (Akron, OH). The volume weighted mean particle size of sulfur particles in water was ~ 2.9 μm and the number weighted mean particle size was ~ 0.32 μm. The solid content of Bostex 410 was ~ 70%.

Preparation of elastomer composites

In this study, a freeze-drying and compression molding method was used instead of a casting method, because there is a density difference between DSF and CB. Using a casting method may produce a less homogeneous sample due to different precipitation

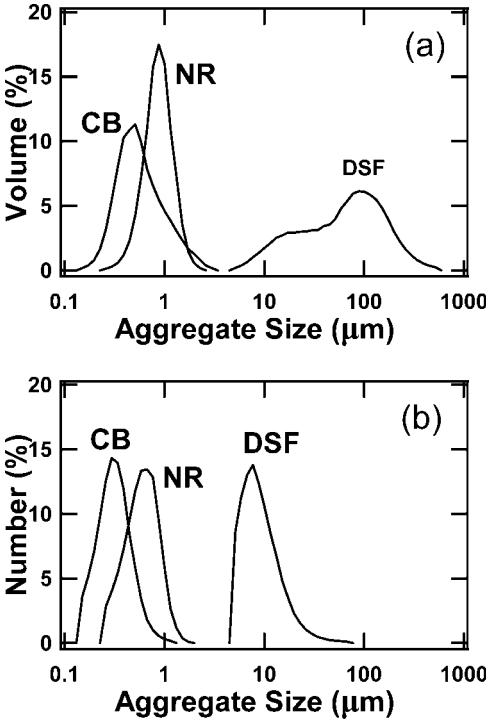

Figure 1 Aggregate size of CB, NR latex, and DSF: (a) volume distribution (b) number distribution.

rates of DSF and CB. For this study, DSF was first dispersed in water at ~ 10% concentration, pH~10, and 55°C for 1 h. The cooled DSF dispersion was then blended homogeneously with CB dispersion at three different dry weight ratios (1 : 3, 1 : 1, and 3 : 1). The NR latex, already adjusted to pH 10, was then added to the filler mixture and mixed homogeneously to form composites with three different filler contents (20 wt %, 30 wt %, and 40 wt %). 3 phr of sulfur in the form of 29% dispersion was added and mixed homogeneously. The homogeneous composite mixtures were then quickly frozen in a rotating shell freezer at about −40°C, followed by freeze-drying in a freeze-dryer (LABCONCO, Kansas City, MO). The moisture content of dried composite crumb is <2%. The freeze-dried crumb was compression molded in a plunge type mold at 69 MPa and 140°C for 2.5 h. After compression molding, the samples were relaxed and further annealed at 80, 110, and 140°C for 24 h, respectively. The torsion bars of 100% NR and DSF were prepared by the same process as that of the co-filler composites. The dried samples had moisture contents <0.8% as measured by halogen moisture analyzer (Mettler Toledo HR73) at 105°C for 60 min. For comparison, DSF and CB composites were prepared using the same procedure as that of co-filler composites. The densities of DSF, CB, and NR were measured by using a density bottle with a low viscosity poly(dimethylsiloxane) as the immersion liquid.

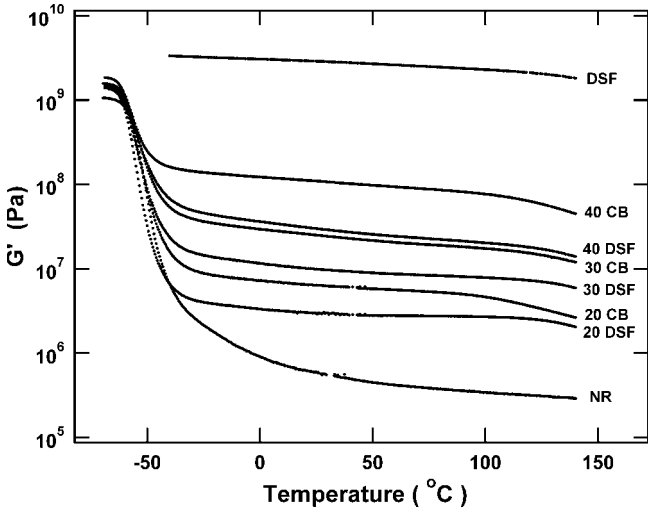

Figure 2 Storage moduli of DSF/NR and CB/NR composites. The weight fraction of fillers is indicated at the end of each curve.

Dynamic mechanical measurements

A rheometric ARES-LSM rheometer (TA Instruments, Piscataway, NJ) was used in the dynamic mechanical measurements. By using TA Orchestrator software v 7.1.2.3, temperature ramp experiments were conducted using torsion rectangular geometry with a heating rate of 1°C/min in a temperature range from −70 to 140°C. When using torsion rectangular geometry, torsional bars with dimensions of approximately 40 × 12.5 × 5 mm^3 were mounted between a pair of torsion rectangular fixtures and the dynamic mechanical measurements were conducted at a frequency of 0.16 Hz (1 rad/s) and a strain of 0.05%.

For the strain sweep experiments, the oscillatory storage and loss moduli, $G'(\omega)$ and $G''(\omega)$, were measured using a torsional rectangular geometry. The shear strain-controlled rheometer is capable of measuring the oscillatory strain down to 3×10^{-5} % strain (TA Instruments, Piscataway, NJ). The rheometer was calibrated in terms of torque, normal force, phase angle, and strain using the instrument procedure. A rectangular sample with dimension of approximately 12.5 × 20 × 5 mm^3 was inserted between the top and bottom grips. The gap between the fixtures was ~ 8 mm to achieve a strain of ~ 20%. A sample length shorter than 5 mm is not desirable because of the shape change from the clamping at both ends of the sample. The frequency used in the measurements was 1 Hz. The oscillatory storage and loss moduli were measured over a strain range of approximately 0.007–20%. The actual strain sweep range was limited by sample geometry and motor

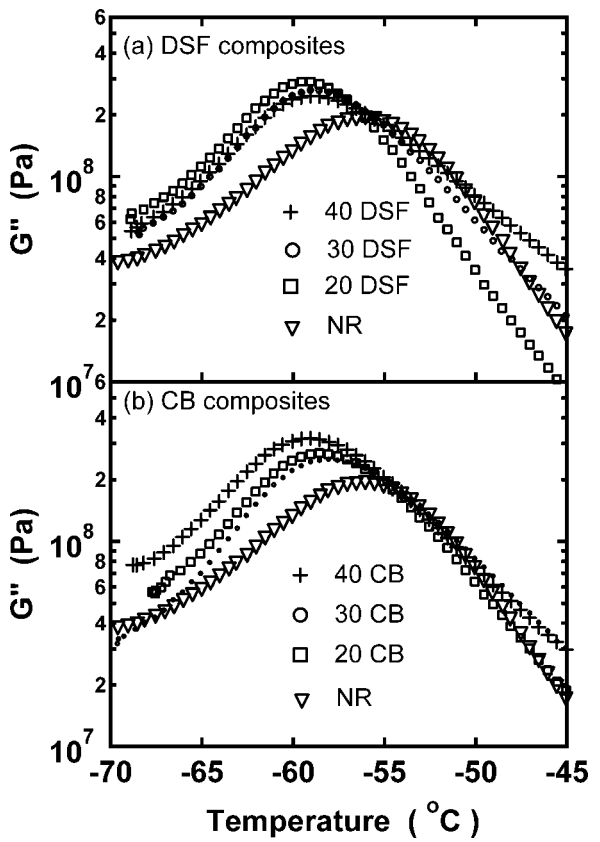

Figure 3 Loss moduli of DSF/NR and CB/NR composites. The filler fractions are indicated in the graphs.

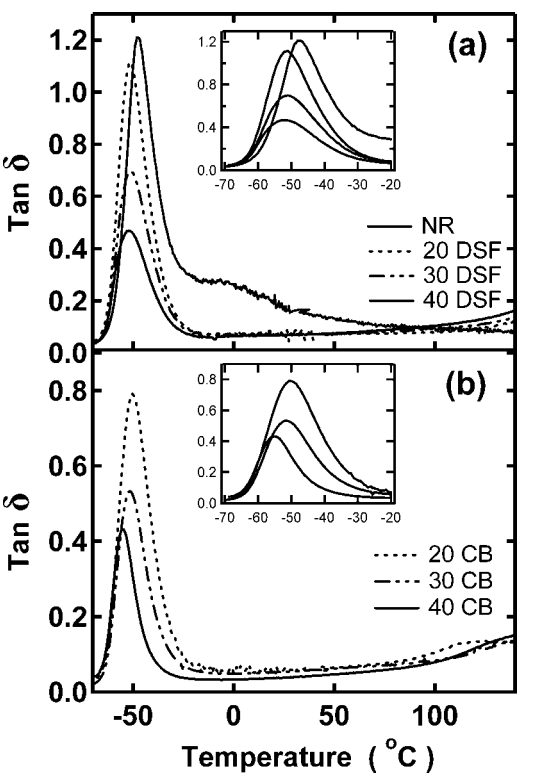

Figure 4 Loss tangent of DSF/NR and CB/NR composites. The filler fractions are indicated in the graphs.

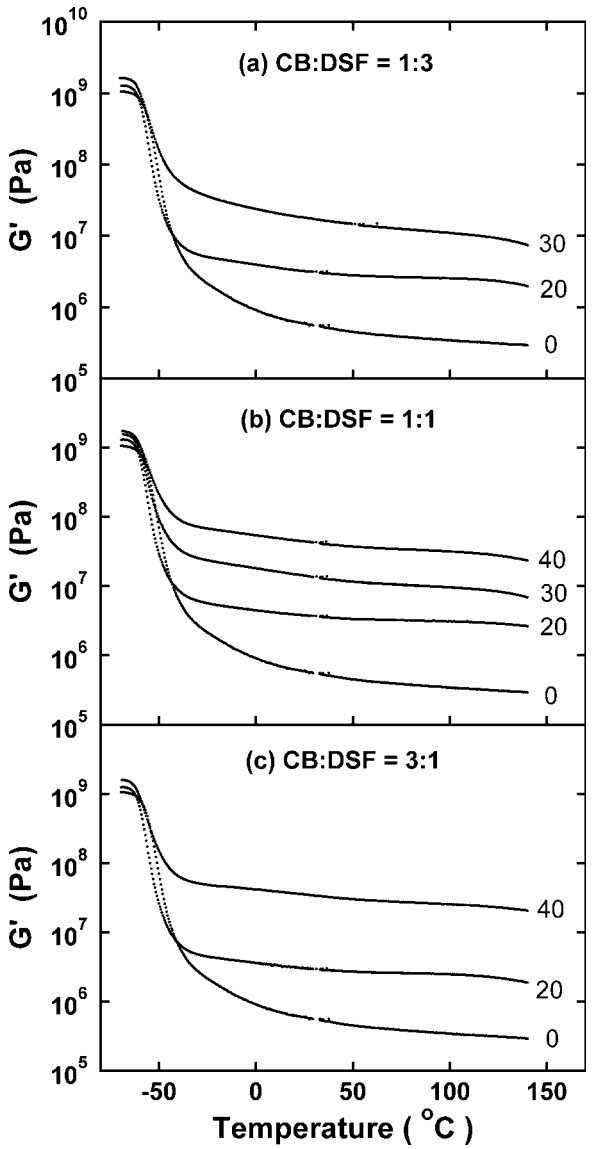

Figure 5 Elastic moduli of co-filler composites. The weight fraction of co-filler is indicated at the end of each curve. The co-filler ratios are indicated in the graphs.

compliance at large strain, and transducer sensitivity at small strain. The data that was out of the transducer range was rejected. Although harmonics in the displacement signal may be expected in a nonlinear material, a previous study[17] indicated that the harmonics are not significant if the shearing does not exceed 100%. Each sample was conditioned at 100°C for 30 min and then subjected to 8 cycles of dynamic strain sweep to study the stress softening effect. The delay between strain cycles was 100 s. For clarity, only data from the first, fourth, and eighth cycles are presented in the figures. To measure the recovery behavior at 100°C, G'_0 of the samples was first measured at 0.05% strain and 0.16 Hz (1 rad/s). The samples were subjected to a large strain of 10% for 30 s, followed by periodic measurements of G' at 0.05% strain and 0.16 Hz (1 rad/s) to record the recovered modulus.

RESULTS AND DISCUSSION

Small strain properties of DSF and CB composites

The elastic moduli of DSF and CB composites prepared by the freeze-drying method are shown in Figure 2. In this study, the range of filler fractions in the composites is above the percolation threshold, which means the fillers can form a network due to the presence of a sufficient number of filler aggregates in the rubber matrix. At 100°C, the composite filled with 40% DSF exhibited about 60-fold increase

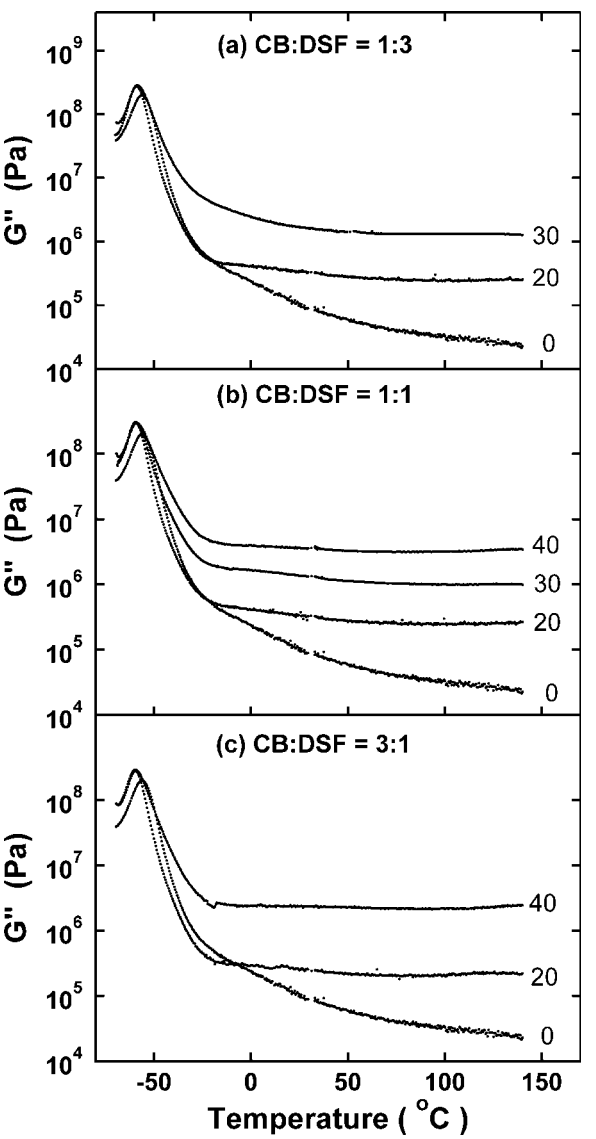

Figure 6 Loss moduli of co-filler composites. The weight fraction of co-filler is indicated at the end of each curve. The co-filler ratios are indicated in the graphs.

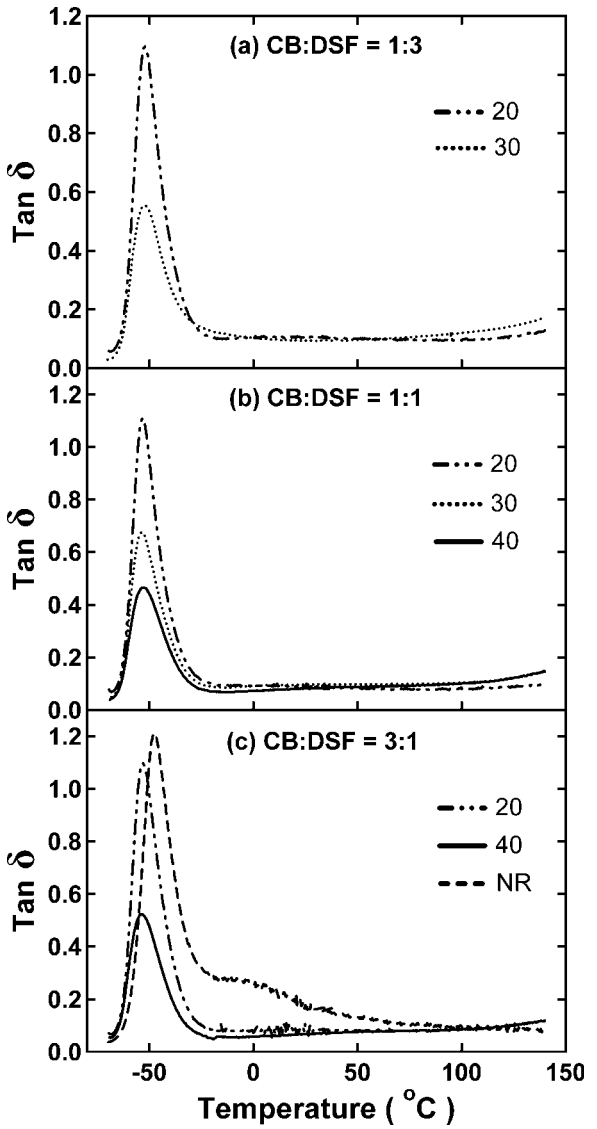

Figure 7 Loss tangent of co-filler composites. The weight fraction of co-filler is indicated at the end of each curve. The co-filler ratios are indicated in the graphs.

in the G' compared with the unfilled NR. For all filler concentrations, DSF composites have a lower G' than CB composites within the rubber plateau region. This is contrary to the carboxylated SB composites reported earlier.[4] The comparison is based on the weight fraction of filler, which is relevant to the economic value of the filler. DSF has a density of 1.41 g/cm^3 and CB has a density of 1.73 g/cm^3. Therefore, DSF has a greater volume fraction than CB at the same weight fraction and the reinforcement effect is proportional to the volume fraction instead of the weight fraction. However, other factors such as the aggregate size of the filler, filler–filler interactions, and filler–rubber interactions also contribute to the observed modulus behavior. The number average size of dry DSF is $\sim$ 6 μm after correcting for the swelling effect in water. The number average size of CB aggregates is $\sim$ 0.3 μm. This result indicates that DSF in the NR matrix does follow the conventional concept that larger particles have less reinforcement effect, other factors being equal. Compared with the particle size of SB latex ($\sim$ 0.18 μm) used in the previous study, NR latex has a larger particle size ($\sim$ 0.85 μm). The larger particle size may lead to a less dense packing with DSF particles and result in a reduction of particle contact area. Another difference between NR and SB latex is the ionic functional groups. Carboxylated SB has more ionic functional groups than NR. This may lead to different interaction strength between DSF and NR. Both latex particle size and ionic functional groups appear to be possible causes in reducing the DSF and NR interactions and result in a lower modulus when compared to carboxylated SB composites reported earlier.[4]

Figure 3 shows that the addition of filler to NR matrix also shifted the glass transition temperature of the composites to a lower temperature compared to that of crosslinked NR. Both DSF and CB composites exhibited the same tendency. This may be due to the reduction of crosslinking points when the presence of filler disrupts interpolymer chain interactions in NR. Figure 4 shows that a hump at $\sim$ 0°C in NR disappears as the fillers are incorporated into the NR matrix, indicating the disruption of polymer chain–chain interactions by the fillers.

Small strain properties of co-filler composites

Figure 5 shows G' of co-filler composites with three different co-filler ratios. The general features of G'

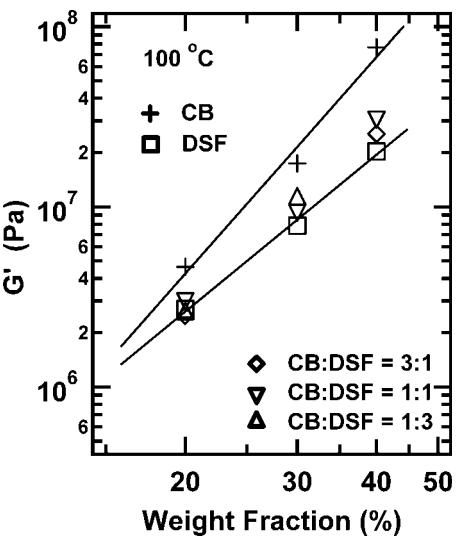

Figure 8 Elastic moduli of co-filler composites at 100°C. The DSF and CB composites are also included for comparison.

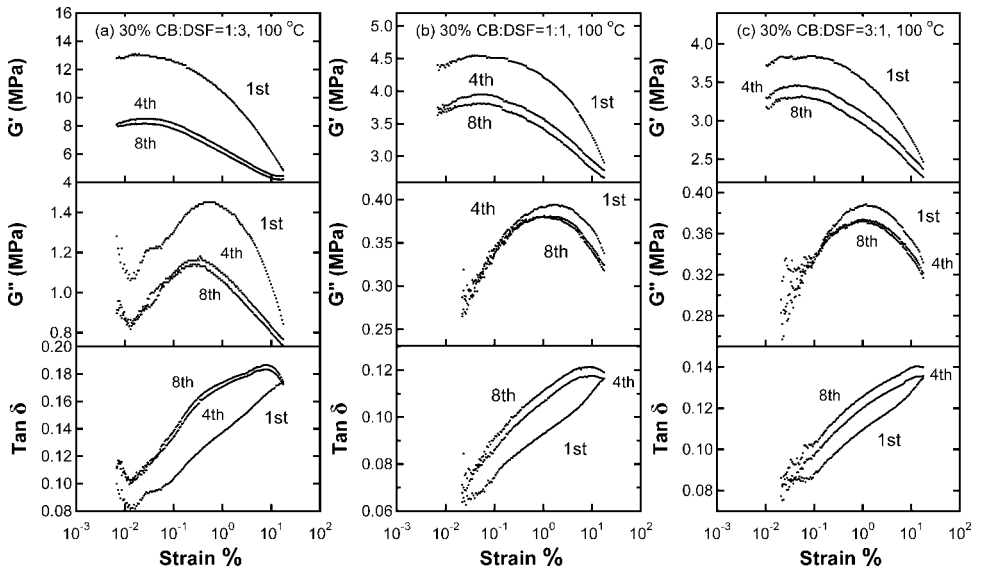

Figure 9 Strain sweep experiments of composites reinforced by 30 wt % co-filler at 100°C. Co-filler ratios are indicated in the graphs. Only 1st, 4th, and 8th strain cycles are shown.

over the entire temperature range for the three different co-filler ratios are similar. G'' of co-filler composites is shown in Figure 6. No shifting of G'' maximums with co-filler concentration are observed for co-filler composites when disregarding the ratio of DSF and CB. The shifting of the G'' maximum of co-filler composites to a lower temperature compared with that of NR is similar to that of the DSF or CB filled composites in Figure 3. The damping behavior of these co-filler composites are shown in Figure 7, and it follows a general trend of decreasing value as filler concentration is increased. In the rubbery

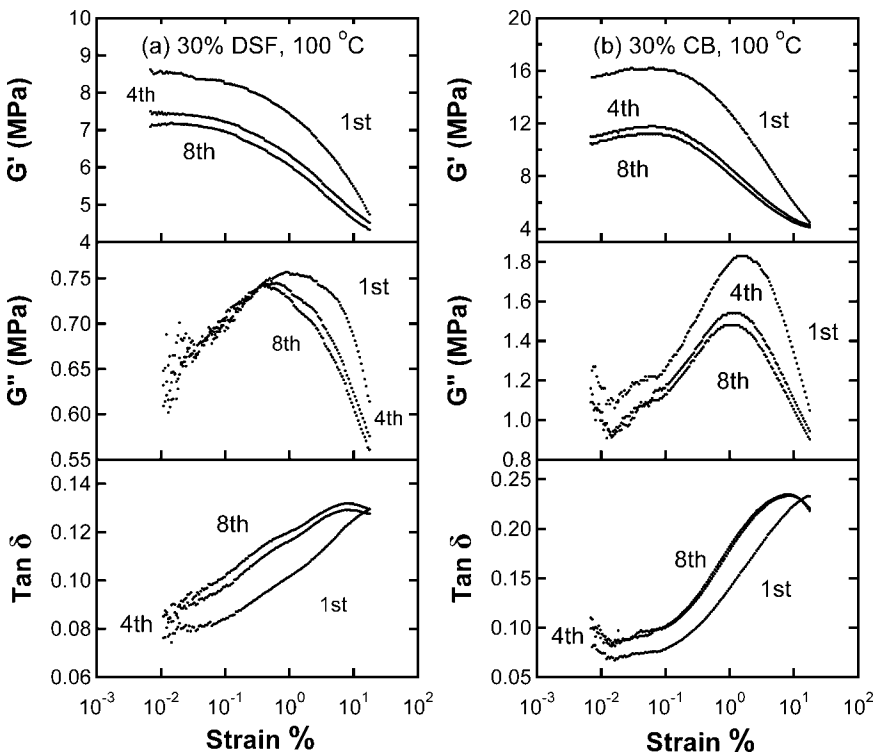

Figure 10 Strain sweep experiments of composites reinforced by 30 wt % DSF or CB at 100°C. Only 1st, 4th, and 8th strain cycles are shown.

region, the tan δ values at 25°C for all co-filler composites are in the range of 0.07–0.11, which is slightly higher than the tan δ values of the CB composites (0.04–0.06) and DSF composites (∼ 0.07) shown in Figure 4. The magnitude of tan δ has practical importance in tire applications. A rubber composite that has a smaller tan δ value tends to have a reduced rolling resistance and save energy, while a larger tan δ tends to have an improved skid resistance and wet grip. The ability of DSF to absorb some moisture in a wet state tends to reduce G' and increase tan δ, leading to better wet traction.

For practical purposes, the elastic moduli of all co-filler reinforced composites are summarized in Figure 8. The elastic moduli of co-filler composites were between the boundaries set by the DSF and CB composites. Compared with CB composites prepared by the same procedure, all co-filler composites show a lower elastic modulus in the rubber plateau region. This indicates that the substitution of CB with more economical DSF leads to a reduction in the total filler cost, but also a reduction in the elastic modulus of the composite. Compared with DSF composites, the co-filler reinforced composites have a higher elastic modulus.

Stress softening

The stress softening effect of co-filler composites is shown in Figure 9. The retention of G' in the small strain region can be used to evaluate the instant recovery behavior after the eight cycles of strain deformation. Thus, the G' at 0.05% strain in the eighth cycle of the composites shown in Figure 9(a–c) retains 63%, 84%, and 87% of their first cycles, respectively. It appears that the instant recovery of co-filler composites improves with the increasing CB content. The trend also shows that the instant recovery improves with decreasing co-filler volume fraction because CB has a higher density than DSF. However, when compared with the retention of ∼ 85% G' [Fig. 10(a)] for the DSF composite and ∼ 70% G' [Fig. 10(b)] for the CB composite, the instant recovery of co-filler reinforced composites does not follow a simple additive rule of individual fillers. This indicates a complicated behavior of filler–filler interactions and the formation of filler related network structures. The recovery curves in Figure 11 indicate that the composites with a lower co-filler concentration tend to have better recovery behavior. Comparing Figure 11(a,c), the co-filler composites with a higher CB content tend to have a better instant recovery behavior. These recovery behaviors in co-filler composites also can not be simply explained based on the properties of CB and DSF composites shown in Figure 12, which shows that the DSF composites have a better instant recovery behavior than CB composites, but CB composites have a better final recovery behavior. Another interesting observation is in Figure 12(a), which shows that the CB composites recovered and exceeded their original moduli ($G'/G'_0 > 1$). This phenomenon was also observed previously in SB composites prepared by the freeze-drying method.[18] The samples produced by this method are in a homogeneous state, but is not necessarily in an equilibrium state. The perturbation of composite structure by a large strain forces the filler structure to rearrange and form a slightly stronger structure through the improved connectivity between filler aggregates. This also implies a strain-induced diffusive movement of smaller CB aggregates in a soft rubber matrix.

For loss modulus under consecutive strain cycles, the energy dissipation processes of 1 : 3, 1 : 1, and 3 : 1 co-filler composites (Fig. 9) became less pronounced and the maximums were shifted from

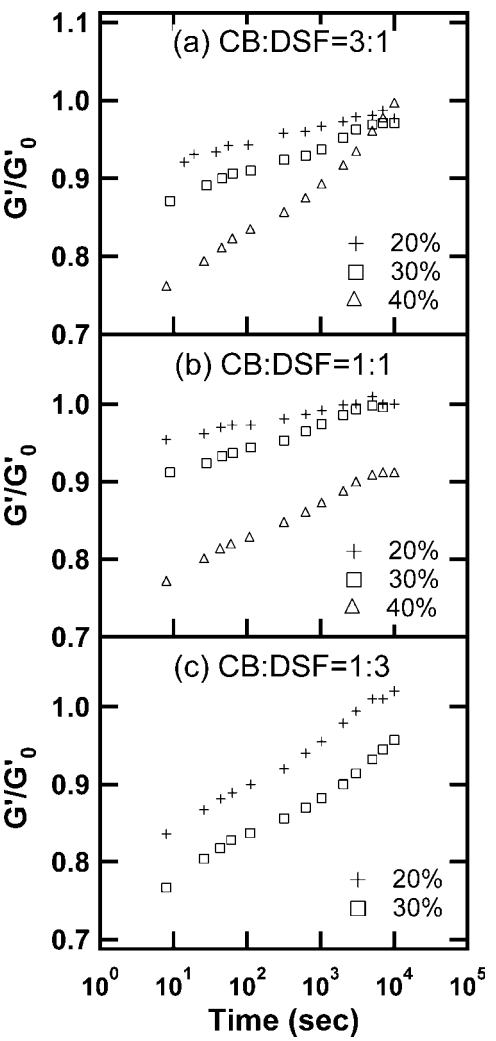

Figure 11 Modulus recovery of co-filler composites measured at 100°C.

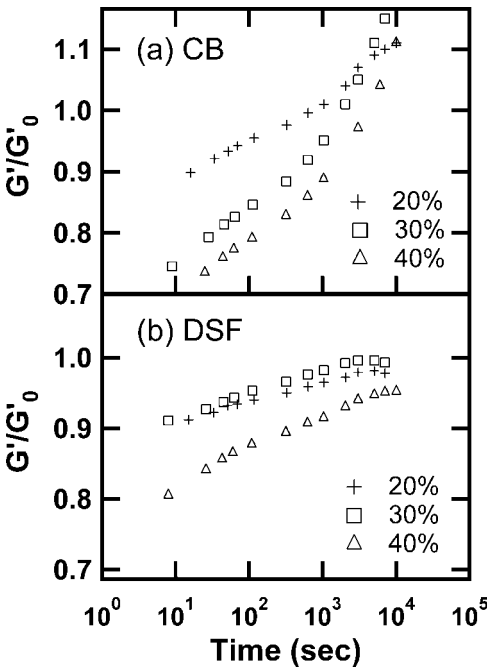

Figure 12 Modulus recovery of CB and DSF composites measured at 100°C.

~ 0.55% strain, ~ 1.76% strain, and ~ 1.17% strain to ~ 0.26% strain, ~ 0.99% strain, and ~ 0.93% strain, respectively. This indicates a co-filler composite with a higher DSF content is less flexible and its G'' maximum occurs at a lower strain. A loss maximum of a composite that occurs at a higher % strain indicates a more elastic structure, which requires a greater extent of deformation to break down the filler related structures. The G' maximums in Figures 9 and 10 are similar to the previous observation on the soy protein filled rubber composites and are attributed to the breaking down of filler immobilized polymer networks.[7]

For the loss tangent properties, the magnitude of tan δ for the co-filler composites within the strain range measured is greater in the composite with a higher DSF content. This behavior is also not predictable from the DSF and CB composites in Figure 10, where the DSF composite has a lower tan δ value than the CB composite. This indicates a partial substitution of CB with DSF can reduce tan δ in the larger strain region. This behavior, however, is different from tan δ in the small strain region at 25°C discussed earlier, where both DSF and co-filler composites show a greater tan δ than the CB composites.

Elasticity of DSF related rubber structures

The reduction of shear elastic modulus with increasing strain is a familiar phenomenon reported by Payne[19–21] on CB filled rubbers in the early 1960s. Later Kraus[22] proposed a phenomenological model based on Payne's postulation of filler networking. The model is based on the aggregation and de-aggregation of CB agglomerates. In this model, the CB contacts are continuously broken and reformed under a periodic sinusoidal strain. On the basis of this kinetic aggregate forming and breaking mechanism at equilibrium, elastic modulus was expressed as follows:

$$\frac{G'(\gamma) - G'_\infty}{G'_0 - G'_\infty} = \frac{1}{1 + (\gamma/\gamma_c)^{2m}} \quad (1)$$

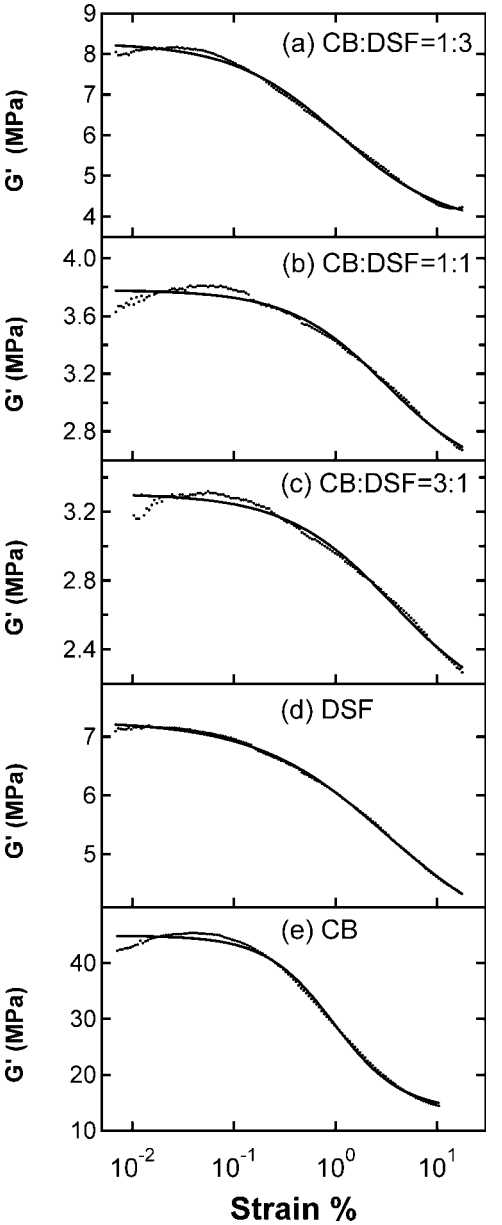

Figure 13 30% filled composites. The 8th cycle of strain sweep experiments at 100°C and 1 Hz. Solid lines are the fit from the Kraus model.

TABLE I
Fitting Parameters of Shear Elastic Modulus[a]

Composition	Best fit[b] (m)	γ_c (%)	G'_0 (MPa)	G'_∞ (MPa)
30% filler				
DSF	0.33 ± 0.02	3.22 ± 0.47	7.27 ± 0.03	3.38 ± 0.19
CB	0.65 ± 0.06	0.96 ± 0.08	44.9 ± 0.44	13.6 ± 1.19
30% Co-filler				
CB : DSF = 1 : 3	0.41 ± 0.03	1.08 ± 0.12	8.28 ± 0.07	3.74 ± 0.18
CB : DSF = 1 : 1	0.46 ± 0.07	3.19 ± 0.97	3.78 ± 0.02	2.46 ± 0.16
CB : DSF = 3 : 1	0.41 ± 0.07	3.75 ± 1.47	3.31 ± 0.03	2.01 ± 0.02
20% Co-filler				
CB : DSF = 1 : 3	0.40 ± 0.06	3.65 ± 1.28	1.67 ± 0.01	1.21 ± 0.06
CB : DSF = 1 : 1	0.44 ± 0.09	5.98 ± 3.27	1.75 ± 0.01	1.39 ± 0.08
CB : DSF = 3 : 1	0.35 ± 0.05	5.71 ± 2.29	2.13 ± 0.01	1.32 ± 0.11

[a] The data are from the 8th strain cycle measured at 100°C.
[b] Best fit of shear elastic modulus vs. strain with the Kraus Model.

where G'_∞ is equal to $G'(\gamma)$ at very large strain, G'_0 is equal to $G'(\gamma)$ at very small strain, γ_c is a characteristic strain where $G'_0 - G'_\infty$ is reduced to half of its zero-strain value, and m is a fitting parameter related to the filler aggregate structures. Equation (1) has been shown to describe the behavior of $G'(\gamma)$ in CB filled rubber reasonably well.[15] The loss modulus and loss tangent, however, do not have good agreement with experiments,[23] mainly due to the uncertainty in the formulation of a loss mechanism. In this study, an empirical fit is useful to show the difference in the strain behaviors (Fig. 13 and Table I) of different composites. In general, a smaller fitting parameter m indicates a smooth and continuous decrease of G' with increasing strain and suggests a continuous breaking up of the filler network structure as the strain is increased. On the other hand, a larger m indicates a stronger structure, which does not yield until a certain strain is exceeded. A smaller γ_c value indicates that the filler related network structure is less elastic and breaks down substantially at smaller strain. From Figure 13 and Table I, applying the Kraus model is generally acceptable except when a G' maximum in the small strain region prevents a good fit. For both 20 and 30% co-filler composites, an m value of $\sim$ 0.4 is between those of 30% DSF and 30% CB composites. Comparing γ_c values in Table I between 30% DSF and 30% CB composites, the CB composite is stronger but also breaks down substantially at a lower strain. The 30% DSF composite has a lower modulus, but its structure yields continuously and has a larger γ_c. Co-filler composite behavior however can not be predicted from the separate yield behaviors of 30% DSF and 30% CB composites because they show that a 30% co-filler composite with a higher content of CB actually has a larger γ_c. Comparing 20 and 30% co-filler composites, 20% co-filler composites have a larger γ_c, indicating the effect of increasing amount of rubber matrix on γ_c values. Therefore, the variation of γ_c values in 30% co-filler composites may be due to a different amount of rubber matrix being incorporated into the co-filler network structure as the co-filler ratio varies.

CONCLUSIONS

At 100°C, the composite filled with 40% DSF exhibited roughly a 60-fold increase in G' compared to unfilled NR. For all filler concentrations, DSF composites have a lower G' than CB composites within the rubber plateau region. This is contrary to the carboxylated SB composite results reported earlier. The addition of both DSF and CB filler shifted the glass transition temperature of NR to a lower temperature, indicating an increase of chain mobility in the presence of filler within the glassy temperature region. DSF and CB were used as co-filler at three different ratios in NR matrices. The elastic moduli of co-filler composites are between those of the DSF and CB composites. Both stress softening and recovery experiments indicate that the co-filler composites tend to have a better instant recovery in elastic modulus when CB content in the composites is higher. The observation, however, can not be simply explained based on the recovery behaviors of the single filler (DFS and CB) composites, which show DSF has a better instant recovery, consistent with the instant recovery behavior of the stress softening experiments. The CB composites show that the recovered moduli exceed the original moduli, indicating a nonequilibrium behavior of homogeneous samples prepared by the freeze-drying method. Fitting of strain sweep experiments with the Kraus model indicated that the co-filler composites with a higher CB content are more elastic, which was consistent with the recovery experiment. This study shows that the use of DSF in NR composites does not yield a higher modulus than similarly prepared

CB composites. However, the low cost of DSF and its co-filler composites still provide substantial reinforcement effects when compared with NR alone, and therefore have a potential in certain composite applications.

The author thanks various industrial companies mentioned in the materials section for supplying materials used in this study, and Dr. S. C. Peterson for proofreading this manuscript.

References

1. Ismail, H.; Jaffri, R. M.; Rozman, H. D. J Elastomers Plast 2003, 35, 181.
2. Nair, K. G.; Dufresne, A. Biomacromolecules 2003, 4, 666.
3. Ismail, H.; Shuhelmy, S.; Edyham, M. R. Eur Polym J 2001, 38, 39.
4. Jong, L. J Appl Polym Sci 2005, 98, 353.
5. Jong, L. Polym Int 2005, 54, 1572.
6. Jong, L. Composites: Part A 2006, 37, 438.
7. Jong, L. J Polym Sci Part B: Polym Phys 2005, 43, 3503.
8. Coughlin, E. T. A. U.S. Pat. 2,056,958 (1936).
9. Isaacs, M. R. U.S. Pat. 2,127,298 (1938).
10. Lehmann, R. L.; Petusseau, B. J.; Pinazzi, C. P. U.S. Pat. 2,931,845 (1960).
11. Fuetterer, C. T. U.S. Pat. 3,113,605 (1963).
12. Beckmann, O.; Teves, R.; Loreth, W. Ger. Offen. DE 19622169 A1 19961212 (1996).
13. Recker, C. Eur. Pat. Appl EP 1234852 A1 20020828 (2002).
14. Wang, M. J Rubber Chem Technol 1998, 71, 520.
15. Heinrich, G.; Kluppel, M. Adv Polym Sci 2002, 160, 1.
16. Carter, C. M.; Cravens, W. W.; Horan, F. E.; Lewis, C. J.; Mattil, K. F.; Williams, L. D. In Protein Resources and Technology; Milnre, M.; Scrimshaw, N. S.; Wang, D. I. C., Eds., AVI Publishing: Connecticut, 1978; Chapter 17.
17. Chazeau, L.; Brown, J. D.; Yanyo, L. C.; Sternstein, S. S. Polym Compos 2000, 21, 202.
18. Jong, L. Composites: Part A 2007, 38, 252.
19. Payne, A. R. J Appl Polym Sci 1962, 6, 57.
20. Payne, A. R. J Appl Polym Sci 1962, 6, 368.
21. Payne, A. R. J Appl Polym Sci 1963, 7, 873.
22. Kraus, G. J Appl Polym Sci Appl Polym Symp 1984, 39, 75.
23. Ulmer, J. D. Rubber Chem Technol 1995, 69, 15.